Seasonal and vertical dynamics in the trophic structure of a temperate zooplankton assemblage

Sonia Romero-Romero*[1,a], Ricardo González-Gil[2], Carlos Cáceres [2,b], José Luis Acuña[1]

[1] Área de Ecología, Dpto. de Biología de Organismos y Sistemas, Universidad de Oviedo, Catedrático Rodrigo Uría s/n, 33071 Oviedo, Asturias, Spain

[2] Department of Mathematics and Statistics, University of Strathclyde, Glasgow, UK

[a] Present address: University of Hawaii at Manoa, Department of Oceanography, 1000 Pope Road, Honolulu, Hawaii, 96822, USA

[b] Present address: Schiermeier Olentangy River Wetland Research Park, School of Environment and Natural Resources, The Ohio State University, Columbus, USA

*Corresponding author: romeroromerosonia@gmail.com

Running head: Trophic structure of zooplankton

Abstract

We determined the stable nitrogen isotope composition (δ^{15}N values) and body size of taxonomic groups in a zooplankton community in the Cantabrian Sea (southern Bay of Biscay) to explore seasonal and depth (0-2000 m) variations in the size-based trophic structure, and their coupling to the production cycle. The positive linear relationship between δ^{15}N values and log-transformed body size reflects the dominance of new vs. regenerated production. The slope of the relationship (*b)* is high during productive periods and low when herbivory declines and the food web is more dependent on recycled production. This variation can be attributed to high δ^{15}N values of the smallest plankton after repetitive cycles of microbial degradation. Downward transport of organic matter after the spring phytoplankton bloom was captured by a steady variation from low values of *b* at the surface to high values at the bathypelagic zone, where the imprint of the spring production pulse could still be detected. Variation in *b* reveals that the meso- and bathypelagic zooplankton communities are as dynamic as their epipelagic counterparts. This shows the efficiency of δ^{15}N vs. body size relationships to capture fast, transient ecosystem processes without need for lengthy incubations or complex rate measurements.

Keywords: deep-sea, stable isotopes, size-based

Introduction

Deep benthic communities depend on a "rain" of organic matter (OM) produced at the surface of the ocean and transported downwards by a combination of mechanisms known as the "biological pump" (Turner 2015). To reach the deep ocean floor, the OM must go through the mesopelagic zone, where nearly 90% of the exported carbon is respired (Arístegui et al. 2005). Passively sinking particulate organic carbon is regarded as the main source of organic carbon to the deep-sea. However, zooplankton alter the carbon flux by consuming and metabolizing sinking or suspended particles and by fragmenting large aggregates (Dilling and Alldredge 2000), or by repackaging the ingested particles into fecal pellets (Wilson et al. 2008). In addition, they perform diel vertical migrations, which contribute to the rapid descent of fecal pellets, molts, and dead carcasses to deeper portions of the water column (Steinberg et al. 2008; Burd et al. 2010). Zooplankton also represent the trophic link between phytoplankton and higher trophic levels (Hannides et al. 2009), thus a change in the trophic structure of zooplankton may potentially affect the entire food web. Although the structure and dynamics of zooplankton are of major importance to the functioning of deep-sea ecosystems, their study, especially in the deep-sea, has been hindered by sampling constraints at representative time and space scales (Robinson et al. 2010).

Seasonal fluctuations in primary production, especially accentuated in temperate seas with a marked annual cycle, are determinant for the dynamics of the deep ocean (Gooday 2002). In these temperate regions, the transition from mixed to stratified conditions in spring and back to mixing in autumn releases phytoplankton cells from

light/nutrient limitation, leading to two major production pulses known as the spring and autumn blooms, respectively (e.g. Fernández and Bode 1991; González-Gil et al. 2018). Stratification favors the prevalence of a microbial food loop (Cushing 1989; Legendre and Rassoulzadegan 1995), where heterotrophic bacteria recycle the organic matter while feeding a complex community of heterotrophic or mixotrophic microbes, protozoans and copepods (Azam et al. 1983). In contrast, during blooms, the production depends on phytoplankton (Cushing 1989), and the organic matter produced is either efficiently transferred to upper trophic levels in a few trophic steps or rapidly sinks to the deep ocean. Due to difficulties in experimentation and rate measurements at great depths, the impact of seasonal fluctuations in the primary production of the euphotic layer on the trophic structure of deep zooplankton communities remains poorly known.

Stable isotopes are widely used as tracers in studies of trophic ecology to provide information on the origin of organic matter and its transfer through the food web (e.g. Boecklen et al. 2011 and references therein). Stable nitrogen isotope values (as δ^{15}N values) are used to estimate the relative trophic level of organisms since they increase ~3-4 ‰ between a predator and its prey (Minagawa and Wada 1984). Additionally, for primary producers, it also informs about the origin of the assimilated nitrogen by organisms. Because of its short tissue turnover rate, the variability in the δ^{15}N values of zooplankton have a marked seasonal component (Rolff 2000; Matthews and Mazumder 2005). Seasonal variations have also been described for the stable isotope composition of deep-sea zooplankton (Fanelli et al. 2011), pointing to a connection between surface dynamics and deep zooplankton communities. In this regard, Laakmann and Auel (2010) indicated that

78 regional changes in surface stable isotope values propagate to deep layers and are reflected
79 in deep-sea carnivorous copepods. Moreover, previous studies on the stable isotope
80 composition of zooplankton have described an increase in δ^{15}N values with depth
81 (Koppelmann 2003; Koppelmann et al. 2009; Hannides et al. 2013). However, there is a
82 lack of studies addressing seasonal variations in the isotopic composition of zooplankton
83 simultaneously at different depths.

84 Size-based analyses provide information about the structure and function of a food
85 web (Cohen et al. 1993; Jennings and Dulvy 2005; Woodward et al. 2005), since body size
86 is a key attribute related to many life-history traits (Peters 1983). For instance, predators are
87 usually larger than their prey (Sheldon et al. 1972), which explains why the body size of
88 organisms accounts for more variation in their trophic position than their taxonomic
89 identity (Jennings et al. 2008a). Previous studies have quantified the relationship between
90 body size and trophic level in marine ecosystems using analyses of stable isotopes, and
91 most assumed that the dependence of trophic level on body size is constant through time
92 (e.g. Jennings et al. 2002; Al-Habsi et al. 2008), although there are few investigations
93 where temporal variations were considered (e.g. Jennings et al. 2007; Nakazawa et al.
94 2010; Romero-Romero et al. 2016a). This relationship is expected to be stronger in marine
95 food webs which are based on phytoplankton than those dependent on detritus (Layman et
96 al. 2005; Al-Habsi et al. 2008). If that holds true, dependence of new versus recycled
97 production, which vary during the annual cycle of nutrients, could be reflected in the
98 strength of the relationship between δ^{15}N values and body size, when organisms with short
99 tissue turnover rates are analyzed. However, food web studies using stable isotopes have

100 traditionally been limited to larger-sized organisms (Middelburg 2014) because the analysis
101 of the stable isotope composition of zooplankton requires a pool of organisms, so samples
102 are commonly analyzed according to their size binned in size fractions. This restricts the
103 analysis to typically four or five discrete size classes (e.g. Rolff 2000; Hannides et al.
104 2013), preventing the use of size-based approaches.
105 In this study, we analyzed seasonal variations throughout the water column in the
106 δ^{15}N values of zooplankton according to their taxonomic group. We used a body size-based
107 approach to quantify changes in the dependence of the zooplankton food web in the
108 Cantabrian Sea (southern Bay of Biscay) on new versus recycled production. We
109 hypothesized that the relationship between δ^{15}N values and body size would be stronger
110 during the spring phytoplankton bloom than during the stratification period and that
111 seasonal variations would be less marked at greater depths.
112

113 **Materials and Methods**

114 *Sampling methods* – The study area extended from 44°23' to 43°56' N and from
115 6°31' to 5°47' W (Fig. 1) over the Avilés submarine canyon, which is part of a complex
116 network of canyons and valleys off the Central Cantabrian margin in the Bay of Biscay
117 (Northern Iberian Peninsula; Gómez-Ballesteros et al. 2014). Samples were collected on
118 board the research vessel B/O Sarmiento de Gamboa during three oceanographic cruises:
119 between 3 and 13 March 2012 (BIOCANT1); between 27 September and 6 October 2012
120 (BIOCANT2) and between 24 April and 4 May 2013 (BIOCANT3). During each cruise we
121 sampled at five different stations: C3, C5, C8, TP and P3 as well as at station C6 during

BIOCANT3 (Fig. 1), and obtained profiles of temperature, salinity and fluorescence by means of a Seabird911- plus CTD probe. Water samples for the measurement of chlorophyll *a* (Chl *a*) and particulate organic matter (POM) were collected using Niskin bottles at depths of 5, 25, 50, 75, 100, 200, 300, 500 m, and then every 500 m down to the seafloor at each station (n = 201). Mesozooplankton was collected by oblique tows of a 1 m^2 Multiple Opening/Closing Net and Environmental Sensing System (MOCNESS) equipped with 8 nets of 200 µm mesh size. Tow intervals for the MOCNESS were defined according to the water mass structure (Botas et al. 1989), as depicted in the CTD profiles: 1) Surface Water (SW), which coincides with the mixing layer from 0-200 m depth; 2) North Atlantic Central Water (NACW), from 200 m to the salinity minimum located around 400-500 m depth; 3) Mediterranean Water (MW), which goes down to around 1200 m depth when a salinity of 35.6 is reached; and 4) Transition Water (TW), which is a mixture between MW and deep water and it was sampled only at the deepest stations (C5, C6 and C8) down to 2000 m (Fig. 1).

Sample processing and stable isotope analyses – Water samples for the analyses of suspended POM were prefiltered through a 100 µm mesh sieve to remove mesozooplankton, filtered through 25 mm Whatman GF/F filters and stored frozen at -20°C. Each mesozooplankton sample was divided into two halves using a Motoda splitter, one half was fixed in a 4% formaldehyde sea-water buffered solution and the other half was transferred to Whatman glass-fiber GF/A filters and immediately stored frozen at -20°C. For stable isotope analyses, each zooplankton sample was first thawed and then fractionated through a 500 µm mesh sieve to separate the 200-500 µm size class that was

144 processed as a single sample. Then, individuals larger than 500 µm were sorted according
145 to their taxonomic group and, when possible, 6 to 10 groups from each water mass within
146 each sampling station were separated. Most specimens were determined to genus level
147 (Supporting Information Table S2). To obtain sufficient sample material for stable isotope
148 analysis, several individuals of similar size belonging to the same taxonomic group were
149 pooled together. All individuals within a sample were photographed together under a
150 stereoscopic microscope. From the pictures taken, we determined the mean body length of
151 each sample using the image analysis software ImageJ (Abràmoff et al. 2004) and
152 calculated body mass using length/weight conversion factors available in the literature
153 (Company and Sardà 2000, for decapods; Färber-Lorda 1994, for euphausiids; and Uye
154 1982 for copepods, ostracods, cladocerans and chaetognaths).
155 Prior to isotopic analysis, all POM and zooplankton samples were dried at 60°C for
156 48 h. We did not extract lipids from the samples since lipid extraction has been reported to
157 have little effect on δ^{15}N values of aquatic organisms (Ingram et al. 2007). After drying,
158 GF/F filters were packed in 5×9 mm tin capsules. Zooplankton samples were ground to a
159 fine powder using pestle and mortar and packed in 3.3×5 mm tin capsules. All samples (n=
160 544) were processed in a Thermo Finnigan Mat Delta Plus isotope-ratio mass spectrometer
161 coupled to a Carlo Erba CHNSO 1108 elemental analyzer in the Unidad de Técnicas
162 Instrumentales de Análisis (A Coruña, Spain). ^{15}N abundance is expressed in δ notation as
163 the deviation from the standard in parts per thousand (‰) according to the following
164 equation:

165 $$\delta^{15}N = [(R_{sample}/R_{standard})-1] \times 1000,$$

where R is the ratio $^{15}N/^{14}N$ and the $R_{standard}$ values were based on atmospheric N_2. Measurements of internal laboratory standards glutamic acid (USGS40, USGS41) and L-alanine (IA R041) every 16 samples indicated measurement errors of ± 0.1, 0.2 and 0.14‰ for $\delta^{15}N$, respectively.

Data analysis – To determine the influence of depth and season on the size-based trophic structure we fitted linear mixed effects models. The fitted models were nested in a global model (i.e. highest-dimensioned) that included $\delta^{15}N$ as dependent variable, body size (W) as covariate, depth strata (SW, NACW, MW and TW) and cruise (March 2012, October 2012 and May 2013) as fixed factors, and taxonomic group as random factor (Supporting Information). We used linear mixed effects models to take into account variation due to taxonomic identity, included as random factor. Data from the smallest zooplankton size fraction (200-500 µm) was excluded from the analysis because it integrated a wide size range. We then followed a top-down model selection approach as recommended by Zuur et al. (2009) and ranked models according to their second-order Akaike Information Criterion (AICc). The conditional R^2 value (i.e. variance explained by both fixed and random factors) was calculated following Nakagawa and Schielzeth (2013).

We defined the $\delta^{15}N$ values at the base of the studied food web as the predicted $\delta^{15}N$ for organisms weighing 10^{-4} g from each fitted regression line of the best model. We also analyzed, for those taxonomic groups present in all three BIOCANT cruises, the relationship between their range of variation of $\delta^{15}N$ values among seasons (i.e. highest minus lowest mean $\delta^{15}N$ values) and their mean body size. We performed all statistical

187 analyses using R, version 3.1.3 (R Core Team 2015) and we used the *lme4* package (Bates
188 et al. 2014) to fit the linear mixed models.

189

190 **Results**

191 *Depth changes in the stable isotope composition of size-fractionated zooplankton* –
192 We determined the δ^{15}N values of 343 samples belonging to 39 taxonomic groups
193 (Supporting Information Table S1). The δ^{15}N values of zooplankton, averaged for all size
194 fractions, increased significantly with depth (from SW to TW) for all three cruises
195 irrespective of the sampling station (ANOVA; March: $F_{1,118} = 89.6$, $p < 0.001$, n=120;
196 October: $F_{1,101} = 4.41$, $p = 0.001$, n=103; May: $F_{1,118} = 14.64$, $p < 0.001$, n=120; Fig. 2),
197 with the highest increase during March (BIOCANT 1; 4.1–9.9‰). In October (BIOCANT
198 2), there was a smaller increase of δ^{15}N values with depth (6.6–8.0‰), however
199 zooplankton had on average higher δ^{15}N values than in March, mainly within SW (0-200
200 m). In May (BIOCANT 3), δ^{15}N values increased with depth especially for those organisms
201 >5.0 mm (5.9–10.9‰). For all three cruises, there was also a trend towards higher δ^{15}N
202 values with size fraction within each water mass (Fig. 2). The δ^{15}N values of suspended
203 POM also generally increased with depth, especially in the upper 300 m. However, in
204 March, δ^{15}N values of suspended POM below 500 m were depleted in ^{15}N in relation to
205 surface waters and differed markedly from that of zooplankton. In contrast, in May the δ^{15}N
206 values of suspended POM were similar to those of the smallest zooplankton size fractions
207 throughout the water column.

208 *Size-based trophic structure* – The best linear mixed model explained a variance of
209 80%, and included: body size as covariate; season and depth as fixed factors, with a

different slope and intercept for each level of a factor (i.e. triple interaction between body size, season and depth); and taxonomic group as random factor affecting the intercept (Supporting Information Table S3). The results from the best model are shown in Figures 3 and 4. In March, the slope of the δ^{15}N vs. $\log_{10}$ W relationship (*b)* was highest in SW and shallower at higher depths. The opposite was true in May, when *b* was shallowest at SW and increased towards the deep TW. In contrast, in October *b* was mainly constant throughout the water column. The predicted δ^{15}N values for organisms at the base of the studied food web (i.e. organisms weighing 10^{-4} g) increased markedly with depth in March, whereas in October and especially in May they remained nearly invariant, being higher in October (Fig. 4). Seasonal fluctuations in the δ^{15}N values of taxonomic groups were negatively correlated to their body size (δ^{15}N = 0.19 - 0.68 $\log_{10}$ W; R^2 = 0.31; p = 0.01; n = 18; Supporting Information Fig. S2). Hence, smaller organisms exhibited higher seasonal variations in δ^{15}N values.

Discussion

Our results implied that the onset of nutrient regeneration leaves a clear imprint on the size-based trophic structure of the zooplankton community in a deep oceanic water column. The lack of structure, as revealed by a flat δ^{15}N vs $\log_{10}$ body size line, which is characteristic of a recycling state, appeared at the surface following the spring production peak, and propagated downward following an orderly sequence which could be readily identified at surprisingly short time-scales (Figs. 3 and 4). Certainly, seasonal patterns in the stable isotope composition of zooplankton have previously been described (e.g. Rolff 2000; Matthews and Mazumder 2005; Kürten et al. 2013; Espinasse et al. 2014), including

variations in the relationship between δ^{15}N values and size in epipelagic zooplankton (Rolff 2000). However, ours is the first evidence of seasonal changes in the size-based trophic structure along a depth gradient.

The BIOCANT cruises are representative of three different environmental conditions, which were previously described in Romero-Romero et al. (2016a; Table 1; Supporting Information Fig. S1). Conditions during BIOCANT 1 (March 2012) were typical for the onset of the spring phytoplankton bloom, with high concentrations of Chl *a* that reflected the high, newly produced phytoplankton biomass (González-Gil et al. 2018). During that period, the food web in SW was highly size-structured, as shown by the high *b* (2.37 ‰ g^{-1}; Fig. 3a), suggesting that the herbivorous food web was the dominant trophic pathway in SW. Assuming a constant trophic fractionation of 3.4‰ (Minagawa and Wada 1984), the predator: prey body mass ratio (PPMR) in size-structured food webs can be calculated from *b* as PPMR = $10^{(3.4/\,b)}$ (Jennings et al. 2002), yielding a value of 27:1. This PPMR calculated for zooplankton is two orders of magnitude lower than mean estimates for the entire ecosystem from copepods to top predators (~10^3:1; Romero-Romero et al. 2016a). This might be explained by the fact that PPMR increases with predator size (Barnes et al. 2010) and our analysis was focused only on a narrow size range not including larger organisms. In contrast to the situation in SW, the food web in deeper water masses was less structured because most of the newly produced organic matter in SW had not yet started to sink (Romero-Romero et al. 2016b). Hence, the OM available below SW was scarce and more refractory, probably forcing primary consumers to broaden their diet. It is important

253 to highlight that in TW in March only four samples were analyzed, therefore the slope of
254 the fitted regression line might not represent an actual pattern.

255 Contrary to the bloom situation, BIOCANT 3 (May 2013) corresponded to an early
256 stratification period (Table 1) during which the food web was unstructured in SW but,
257 became progressively size-structured deeper in the water column (Fig. 3b). Phytoplankton
258 biomass in SW during this cruise had already declined after the 2013 spring bloom (Rumín-
259 Caparrós et al. 2016), so herbivory was likely limited. A shallower *b* was probably the
260 result of opportunistic feeding by the larger organisms on microzooplankton or small-sized
261 particles when food is scarce (Fry and Quiñones 1994). Conversely, as a consequence of
262 the arrival of material produced during the phytoplankton bloom at greater depths, food was
263 plentiful and *b* was steeper at TW (2.29 ‰ g^{-1}; Fig. 3b). Likewise, Koppelmann et al.
264 (1999) explained an increase in mesozooplankton biomass in the bathypelagic zone of the
265 NE Atlantic from spring to summer as a consequence of the arrival, at that great depths, of
266 material produced during the phytoplankton bloom. Our results show that the arrival of that
267 material to the deep ocean has also implications for the trophic structure of the bathypelagic
268 zooplankton food web.

269 During BIOCANT 2 (October 2012), which corresponded to a late stratification
270 period (Table 1), the food web was weakly size-structured across the entire water column
271 (Fig. 3c). This concurs with lower mass fluxes to the seafloor than in spring (Rumín-
272 Caparrós et al. 2016) and limited primary production, which leads to a food web mainly
273 dependent on recycled production. In addition, it is precisely in these conditions that the
274 diel vertical migrations of zooplankton are more active (Takahashi et al. 2009), what would

lead to vertical homogenization. Interestingly, we found that the mesopelagic community, occupying NACW and MW, exhibited a more time-invariant size structure than the epi- and bathypelagic communities. Vertical migrations are mainly conducted by mesopelagic fauna that transport OM from the epipelagic to the mesopelagic zone (Angel and Baker 1983). This may represent a mean to fulfil metabolic carbon requirements in the food-limited mesopelagic zone (Steinberg et al. 2008), and leads us to hypothesize that the mesopelagic zone is seasonally more stable due to vertical migration. Another factor contributing to the relative stability in the size structure of the mesopelagic community might be the typically fast sinking fluxes resulting from high production episodes. The bulk of those fluxes probably reach the benthic system, while mostly bypassing the mesopelagic community (Honjo et al. 1982; Deuser 1986).

Marine plankton communities are usually considered highly structured by size due to scale-dependent processes and constraints on the relative masses of predators and their prey (Sheldon et al. 1977; Jennings et al. 2008a). However, there are clear indications that some of the seasonal variation may in fact be due to changes in the species composition (Bode and Alvarez-Ossorio 2004). For this reason, we have applied a mixed modelling approach that accommodates variation due to taxonomic identity into a coherent statistical framework. For example, the deep copepod *Lucicutia* spp. exhibited consistently high and positive residuals from the δ^{15}N vs. $\log_{10}$ W relationship. Their high mean δ^{15}N value (10.8 ± 0.8‰; Supporting Information Table S2) agrees with that of *Lucicutia longiserrata* in the Mediterranean (11.9‰; Koppelmann et al. 2009), which have been explained by a diet including suspended rather than sinking POM (Gowing and Wishner 1998). In our study,

297 the mean δ^{15}N values of suspended POM below SW (200 m) were 6-7‰ in May and
298 October (Fig. 2), corresponding to a difference of one trophic level with *Lucicutia* spp.
299 However, the nitrogen stable isotope composition of faster sinking particles collected in
300 sediment traps, deployed from March 2012 to March 2013 in the study area, was on
301 average 4.3 ± 0.2‰ (Romero-Romero et al. 2016b), thus lending support to a diet based
302 preferentially on suspended POM.

303 Apart from the variability in the strength of size structuring, there were also marked
304 variations of δ^{15}N values at the base of the studied food web (i.e. smallest zooplankton, Fig.
305 4). Because of their shorter tissue turnover times, smaller organisms are expected to exhibit
306 wider seasonal variability in their stable isotope composition (O'Reilly and Hecky 2002),
307 which is confirmed by observations of a negative correlation between the seasonal range of
308 variation in δ^{15}N values and body size (Jennings et al. 2008b; Supporting Information Fig.
309 S2). During the onset of the spring bloom (March), δ^{15}N values of small zooplankton
310 increased significantly with depth (Fig. 4). This matches the described pathways of OM in
311 the study area, with fresh OM available in SW and old, refractory OM that has suffered
312 several cycles of microbial degradation in deeper water masses (Romero-Romero et al.
313 2016b). If the microbial food loop prevails at the base of the food web, small zooplankton
314 is expected to have higher δ^{15}N values (Saino and Hattori 1980; Mintenbeck et al. 2007).
315 However, in the early stratification period (May), δ^{15}N values of the smaller organisms
316 were nearly constant with depth. This is likely due to the presence of relatively fresh
317 organic material left by a wave of sinking biomass travelling across all depths after the
318 spring bloom. During late stratification (October), δ^{15}N values of small zooplankton were

also similar at all depths, but higher than during the early stratification period, which points to a diet more dependent on recycled production as stratification progresses (Bănaru et al. 2013). An interesting pattern in our results was that the slope of the δ^{15}N vs. $\log_{10}$ W relationship appeared to be constrained by the δ^{15}N values at the base of the studied food web (Fig. 4). In other words, when small zooplankton had high δ^{15}N values, the food web was always weakly size-structured. However, if δ^{15}N values of small zooplankton were low the food web tended to be more size-structured because fresh OM was available. Thus, it seems that the degree of size structuring of a food web depends on the dominant trophic pathway (Supporting Information Fig. S3).

The δ^{15}N values of zooplankton are known to increase with depth, a pattern that has been well grounded on studies in the North Pacific (4.6‰ from 0-1000 m; Hannides et al. 2013), the Mediterranean Sea (~7‰ from 0-4000 m; Koppelmann et al. 2009) or the South Atlantic Ocean (6.9‰ from 0-1600 m; Laakmann and Auel 2010) and is also evident in our results (up to 5.8‰ during the onset of the phytoplankton bloom, from 0-2000 m, Fig. 2). This has been attributed to either a ^{15}N enrichment at the base of the food web or a higher trophic level of deep water organisms (Polunin et al. 2001; Hannides et al. 2013). According to our results, both explanations may hold, depending on the recycling state of the system, with the first explanation applying to old regenerative systems (i.e. deep water masses during the onset of the spring phytoplankton bloom) and the second applying to systems which have recently received inputs of fresh OM (i.e. deep water masses during early stratification).

Conclusions

In summary, our size-based approach using stable isotopes reveals seasonal and vertical changes in the trophic structure of a zooplankton food web at short time-scales, reflecting its coupling with the seasonal cycle of primary production and the transfer of OM to the deep-sea. We demonstrate that meso- and bathypelagic zooplankton communities can be as dynamic as their epipelagic counterparts, and exhibit seasonal variations tightly coupled to the particle flux. Our results also provide strong indication that the size-based trophic structure of zooplankton communities reflects the dominance of new vs. regenerated production within the ecosystem and the time elapsed since the onset of regeneration.

Acknowledgements

This study was carried out within the framework of project DOSMARES (ref. CTM2012-2180-CO3-02) from the Ministry of Science and Innovation, Spanish Government to JLA, and from the Ministry of Economy and Competitiveness through the research project ECOMER (ref. MINECO-18-CGL2017-84268-R). SRR was supported by a FPU fellowship (ref. 12/00851) from the Ministry of Education, Culture and Sports. RGG was supported by a Marie Curie-Clarín COFUND fellowship from the Principality of Asturias and the European Union (ACA17-05). We thank Juan Höfer, Axayacatl Molina-Ramírez, Ricardo Anadón, Fernando González-Taboada, Arturo Castellón and all the scientists and the crew of B/O Sarmiento de Gamboa and the Unidad de Tecnología Marina (UTM) for their help with sampling. This is a contribution of the Asturias Marine Observatory.

References

Abràmoff, M. D., P. J. Magalhães, and S. J. Ram. 2004. Image processing with imageJ. Biophotonics Int. **11**: 36–41.

Al-Habsi, S., C. Sweeting, N. Polunin, and N. Graham. 2008. δ^{15}N and δ^{13}C elucidation of size-structured food webs in a Western Arabian Sea demersal trawl assemblage. Mar. Ecol. Prog. Ser. **353**: 55–63. doi:10.3354/meps07167

Angel, M. V, and A. D. C. Baker. 1983. Vertical distribution of the standing crop of plankton and micronekton at three stations in the northeast Atlantic. Deep Sea Res. Part B. Oceanogr. Lit. Rev. **30**: 463. doi:10.1016/0198-0254(83)90213-3

Arístegui, J., S. Agustí, J. J. Middelburg, and C. M. Duarte. 2005. Respiration in the mesopelagic and bathypelagic zones of the oceans, p. 181–205. *In* P.A. Del Giorgio and P.J. Le B. Williams [eds.], Respiration in Aquatic Systems. Oxford. Univ. Press. doi: 10.1093/acprof:oso/9780198527084.003.0010

Azam, F., T. Fenchel, J. Field, J. Gray, L. Meyer-Reil, and F. Thingstad. 1983. The Ecological Role of Water-Column Microbes in the Sea. Mar. Ecol. Prog. Ser. **10**: 257–263. doi:10.3354/meps010257

Bănaru, D., F. Carlotti, A. Barani, G. Gregori, N. Neffati, and M. Harmelin-Vivien. 2013. Seasonal variation of stable isotope ratios of size-fractionated zooplankton in the Bay of Marseille (NW Mediterranean Sea). J. Plankton Res. **36**: 145–156. doi:10.1093/plankt/fbt083

Barnes, C., D. Maxwell, D. Reuman, and S. Jennings. 2010. Global patterns in predator-prey size relationships reveal size dependency of trophic transfer efficiency. Ecology **91**: 222–232. doi:10.1890/08-2061.1

Bates, D., M. Mächler, B. Bolker, and S. Walker. 2014. Fitting Linear Mixed-Effects Models using lme4. **67**. doi:10.18637/jss.v067.i01

Bode, A., and M. Alvarez-Ossorio. 2004. Taxonomic versus trophic structure of mesozooplankton: a seasonal study of species succession and stable carbon and nitrogen isotopes in a coastal upwelling ecosystem. ICES J. Mar. Sci. **61**: 563–571. doi:10.1016/j.icesjms.2004.03.004

Boecklen, W. J., C. T. Yarnes, B. A. Cook, and A. C. James. 2011. On the use of stable isotopes in trophic ecology. Annu. Rev. Ecol. Evol. Syst. **42**: 411–440. doi:10.1146/annurev-ecolsys-102209-144726

Botas, J. A., E. Fernández, A. Bode, and R. Anadón. 1989. Water masses off the Central Cantabrian Coast. Sci. Mar. **53**: 755–761.

Burd, A. B., D. A. Hansell, D. K. Steinberg, and others. 2010. Assessing the apparent imbalance between geochemical and biochemical indicators of meso- and bathypelagic biological activity: What the @$#! is wrong with present calculations of carbon budgets? Deep. Res. Part II Top. Stud. Oceanogr. **57**: 1557–1571. doi:10.1016/j.dsr2.2010.02.022

Cohen, J. E., S. L. Pimm, P. Yodzis, and J. Saldaña. 1993. Body sizes of animal predators and animal prey in food webs. J. Anim. Ecol. **62**: 67–78. doi:10.2307/5483

402 Company, J. B., and F. Sardà. 2000. Growth parameters of deep-water decapod crustaceans
403 in the Northwestern Mediterranean Sea: a comparative approach. Mar. Biol. **136**: 79–
404 90. doi:10.1007/s002270050011

405 Cushing, D. H. 1989. A difference in structure between ecosystems in strongly stratified
406 waters and in those that are only weakly stratified. J. Plankton Res. **11**: 1–13.
407 doi:10.1093/plankt/11.1.1

408 Deuser, W. G. 1986. Seasonal and interannual variations in deep-water particle fluxes in
409 the Sargasso Sea and their relation to surface hydrography. Deep Sea Res. Part A.
410 Oceanogr. Res. Pap. **33**: 225–246. doi:10.1016/0198-0149(86)90120-2

411 Dilling, L., and A. L. Alldredge. 2000. Fragmentation of marine snow by swimming
412 macrozooplankton: A new process impacting carbon cycling in the sea. Deep. Res.
413 Part I Oceanogr. Res. Pap. **47**: 1227–1245. doi:10.1016/S0967-0637(99)00105-3

414 Espinasse, B., M. Harmelin-Vivien, M. Tiano, L. Guilloux, and F. Carlotti. 2014. Patterns
415 of variations in C and N stable isotope ratios in size-fractionated zooplankton in the
416 Gulf of Lion, NW Mediterranean Sea. J. Plankton Res. **36**: 1204–1215.
417 doi:10.1093/plankt/fbu043

418 Fanelli, E., J. E. Cartes, and V. Papiol. 2011. Food web structure of deep-sea
419 macrozooplankton and micronekton off the Catalan slope: Insight from stable
420 isotopes. J. Mar. Syst. **87**: 79–89. doi:10.1016/j.jmarsys.2011.03.003

421 Färber-Lorda, J. 1994. Length-weight relationships and coefficient of condition of
422 *Euphausia superba* and *Thysanoessa macrura* (Crustacea: Euphausiacea) in south

west Indian Ocean during summer. Mar. Biol. **118**: 645–650.

Fernández, E., and A. Bode. 1991. Seasonal patterns of primary production in the Central Cantabrian Sea (Bay of Biscay). Sci. Mar. **55**: 629–636.

Fry, B., and R. Quiñones. 1994. Biomass spectra and stable isotope indicators of trophic level in zooplankton of the northwest Atlantic. Mar. Ecol. Prog. Ser. **112**: 201–204. doi:10.3354/meps112201

Gómez-Ballesteros, M., M. Druet, A. Muñoz, and others. 2014. Geomorphology of the Avilés Canyon System, Cantabrian Sea (Bay of Biscay). Deep Sea Res. Part II Top. Stud. Oceanogr. **106**: 99–117. doi:10.1016/j.dsr2.2013.09.031

González-Gil, R., F. González Taboada, C. Cáceres, J. L. Largier, and R. Anadón. 2018. Winter-mixing preconditioning of the spring phytoplankton bloom in the Bay of Biscay. Limnol. Oceanogr. **63**: 1264–1282. doi:10.1002/lno.10769

Gooday, A. J. 2002. Biological responses to seasonally varying fluxes of organic matter to the ocean floor: A review. J. Oceanogr. **58**: 305–332. doi:10.1023/A:1015865826379

Gowing, M. M., and K. F. Wishner. 1998. Feeding ecology of the copepod *Lucicutia aff. L. grandis* near the lower interface of the Arabian Sea oxygen minimum zone. Deep. Res. Part II **45**: 2433–2459. doi:10.1016/S0967-0645(98)00077-0

Hannides, C. C. S., B. N. Popp, C. Anela Choy, and J. C. Drazen. 2013. Midwater zooplankton and suspended particle dynamics in the North Pacific Subtropical Gyre: A stable isotope perspective. Limnol. Oceanogr. **58**: 1931–1936.

doi:10.4319/lo.2013.58.6.1931

Hannides, C. C. S., B. N. Popp, M. R. Landry, and B. S. Graham. 2009. Quantification of zooplankton trophic position in the North Pacific Subtropical Gyre using stable nitrogen isotopes. Limnol. Oceanogr. **54**: 50–61. doi: 10.4319/lo.2009.54.1.0050

Honjo, S., S. J. Manganini, and J. J. Cole. 1982. Sedimentation of biogenic matter in the deep ocean. Deep. Res. Part I-Oceanographic Res. Pap. **29**: 609–625. doi:10.1016/0198-0149(82)90079-6

Ingram, T., B. Matthews, C. Harrod, T. Stephens, J. Grey, R. Markel, and A. Mazumder. 2007. Lipid extraction has little effect on the δ^{15}N of aquatic organisms. Limnol. Oceanogr. Methods **5**: 338–343. doi:10.4319/lom.2007.5.338

Jennings, S., C. Barnes, J. Sweeting, and N. V. C. Polunin. 2008a. Application of nitrogen stable isotope analysis in size-based marine food web and macroecological research. Rapid Commun. Mass Spectrom. **22**: 1673–1680. doi:10.1002/rcm

Jennings, S., and N. Dulvy. 2005. Reference points and reference directions for size-based indicators of community structure. ICES J. Mar. Sci. **62**: 397–404. doi:10.1016/j.icesjms.2004.07.030

Jennings, S., T. Maxwell, M. Schratzberger, and S. Milligan. 2008b. Body-size dependent temporal variations in nitrogen stable isotope ratios in food webs. Mar. Ecol. Prog. Ser. **370**: 199–206. doi:10.3354/meps07653

Jennings, S., J. A. A. De Oliveira, and K. J. Warr. 2007. Measurement of body size and

463 abundance in tests of macroecological and food web theory. J. Anim. Ecol. **76**: 72–82.
464 doi:10.1111/j.1365-2656.2006.01180.x

465 Jennings, S., J. Pinnegar, N. Polunin, and K. Warr. 2002. Linking size-based and trophic
466 analyses of benthic community structure. Mar. Ecol. Prog. Ser. **226**: 77–85.
467 doi:10.3354/meps226077

468 Koppelmann, R. 2003. Vertical distribution of mesozooplankton and its δ^{15}N signature at a
469 deep-sea site in the Levantine Sea (eastern Mediterranean) in April 1999. J. Geophys.
470 Res. **108**: 8118. doi:10.1029/2002JC001351

471 Koppelmann, R., R. Böttger-Schnack, J. Möobius, and H. Weikert. 2009. Trophic
472 relationships of zooplankton in the eastern Mediterranean based on stable isotope
473 measurements. J. Plankton Res. **31**: 669–686. doi:10.1093/plankt/fbp013

474 Koppelmann, R., and H. Weikert. 1999. Temporal changes of deep-sea mesozooplankton
475 abundance in the temperate NE Atlantic and estimates of the carbon budget. Mar.
476 Ecol. Prog. Ser. **179**: 27–40. doi:10.3354/meps179027

477 Kürten, B., I. Frutos, U. Struck, S. J. Painting, N. V. C. Polunin, and J. J. Middelburg.
478 2013. Trophodynamics and functional feeding groups of North Sea fauna: A combined
479 stable isotope and fatty acid approach. Biogeochemistry **113**: 189–212.
480 doi:10.1007/s10533-012-9701-8

481 Laakmann, S., and H. Auel. 2010. Longitudinal and vertical trends in stable isotope
482 signatures (δ^{13}C and δ^{15}N) of omnivorous and carnivorous copepods across the South
483 Atlantic Ocean. 463–471. doi:10.1007/s00227-009-1332-9

484 Layman, C., K. Winemiller, D. Arrington, and D. Jepsen. 2005. Body size and trophic
485 position in a diverse tropical food web. Ecology **86**: 2530–2535. doi:10.1890/04-1098

486 Legendre, L., and F. Rassoulzadegan. 1995. Plankton and nutrient dynamics in marine
487 waters. Ophelia **41**: 153–172. doi:10.1080/00785236.1995.10422042

488 Matthews, B., and A. Mazumder. 2005. Consequences of large temporal variability of
489 zooplankton δ^{15}N for modeling fish trophic position and variation. **50**: 1404–1414.
490 doi:doi.org/10.4319/lo.2005.50.5.1404

491 Middelburg, J. J. 2014. Stable isotopes dissect aquatic food webs from the top to the
492 bottom. Biogeosciences **11**: 2357–2371. doi:10.5194/bg-11-2357-2014

493 Minagawa, M., and E. Wada. 1984. Stepwise enrichment of ^{15}N along food chains: Further
494 evidence and the relation between δ^{15}N and animal age. Geochim. Cosmochim. Acta
495 **48**: 1135–1140. doi:10.1016/0016-7037(84)90204-7

496 Mintenbeck, K., U. Jacob, R. Knust, W. E. Arntz, and T. Brey. 2007. Depth-dependence in
497 stable isotope ratio δ^{15}N of benthic POM consumers: The role of particle dynamics
498 and organism trophic guild. Deep Sea Res. Part I Oceanogr. Res. Pap. **54**: 1015–1023.
499 doi:10.1016/j.dsr.2007.03.005

500 Nakagawa, S., and H. Schielzeth. 2013. A general and simple method for obtaining R^2 from
501 generalized linear mixed-effects models R.B. O'Hara [ed.]. Methods Ecol. Evol. **4**:
502 133–142. doi:10.1111/j.2041-210x.2012.00261.x

503 Nakazawa, T., Y. Sakai, C. Hsieh, T. Koitabashi, I. Tayasu, N. Yamamura, and N. Okuda.

2010. Is the relationship between body size and trophic niche position time-invariant in a predatory fish? First stable isotope evidence. PLoS One **5**: e9120. doi:10.1371/journal.pone.0009120

O'Reilly, C. M., and R. E. Hecky. 2002. Interpreting stable isotopes in food webs: recognizing the role of time averaging at different trophic levels. Limnol. Oceanogr. **47**: 306–309. doi:10.4319/lo.2002.47.1.0306

Peters, R. H. 1983. The ecological implications of body size, Cambridge University Press.

Polunin, N. V. C., B. Morales-Nin, W. E. Pawsey, J. E. Cartes, J. K. Pinnegar, and J. Moranta. 2001. Feeding relationships in Mediterranean bathyal assemblages elucidated by stable nitrogen and carbon isotope data. Mar. Ecol. Prog. Ser. **220**: 13–23. doi:10.3354/meps220013

Robinson, C., D. K. Steinberg, T. R. Anderson, and others. 2010. Mesopelagic zone ecology and biogeochemistry - A synthesis. Deep. Res. Part II Top. Stud. Oceanogr. **57**: 1504–1518. doi:10.1016/j.dsr2.2010.02.018

Rolff, C. 2000. Seasonal variation in δ^{13}C and δ^{15}N of size-fractionated plankton at a coastal station in the northern Baltic proper. Mar. Ecol. Prog. Ser. **203**: 47–65. doi:10.3354/meps203047

Romero-Romero, S., A. Molina-Ramírez, J. Höfer, and J. L. Acuña. 2016a. Body size-based trophic structure of a deep marine ecosystem. Ecology **97**: 171–181. doi:10.1890/15-0234.1

524 Romero-Romero, S., A. Molina-Ramírez, J. Höfer, G. Duineveld, A. Rumín-Caparrós, A.
525 Sanchez-Vidal, M. Canals, and J. L. Acuña. 2016b. Seasonal pathways of organic
526 matter within the Avilés submarine canyon: Food web implications. Deep Sea Res.
527 Part I Oceanogr. Res. Pap. **117**: 1–10. doi:10.1016/j.dsr.2016.09.003

528 Rumín-Caparrós, A., A. Sanchez-Vidal, C. González-Pola, G. Lastras, A. Calafat, and M.
529 Canals. 2016. Particle fluxes and their drivers in the Avilés submarine canyon and
530 adjacent slope, central Cantabrian margin, Bay of Biscay. Prog. Oceanogr. **144**: 39–
531 61. doi:10.1016/j.pocean.2016.03.004

532 Saino, T., and A. Hattori. 1980. ^{15}N natural abundance in oceanic suspended particulate
533 matter. Nature **283**: 752–754. doi:10.1038/283752a0

534 Sheldon, R. W., A. Prakash, and H. Sutcliffe. 1972. The size distribution of particles in the
535 ocean. Limnol. Oceanogr. **17**: 327–340. doi:10.4319/lo.1972.17.3.0327

536 Sheldon, R. W., W. H. Sutcliffe Jr., and M. A. Paranjape. 1977. Structure of pelagic food
537 chain and relationship between plankton and fish production. J. Fish. Res. Board
538 Canada **34**: 2344–2353. doi:10.1139/f77-314

539 Steinberg, D. K., B. A. S. Van Mooy, K. O. Buesseler, P. W. Boyd, T. Kobari, and D. M.
540 Karl. 2008. Bacterial vs. zooplankton control of sinking particle flux in the ocean's
541 twilight zone. Limnol. Oceanogr. **53**: 1327–1338.
542 doi:doi.org/10.4319/lo.2008.53.4.1327

543 Takahashi, K., A. Kuwata, H. Sugisaki, K. Uchikawa, and H. Saito. 2009. Downward
544 carbon transport by diel vertical migration of the copepods *Metridia pacifica* and

Metridia okhotensis in the Oyashio region of the western subarctic Pacific Ocean. Deep. Res. Part I Oceanogr. Res. Pap. **56**: 1777–1791. doi:10.1016/j.dsr.2009.05.006

Team, R. C. 2015. R: A Language and Environment for Statistical Computing. Vienna, Austria: R Foundation for Statistical Computing.

Turner, J. T. 2015. Zooplankton fecal pellets, marine snow, phytodetritus and the ocean's biological pump. Prog. Oceanogr. **130**: 205–248. doi:10.1016/j.pocean.2014.08.005

Uye, S. 1982. Length-weight relationships of important zooplankton from the inland Sea of Japan. J. Oceanogr. Soc. Japan **38**: 149–158.

Wilson, S. E., D. K. Steinberg, and K. O. Buesseler. 2008. Changes in fecal pellet characteristics with depth as indicators of zooplankton repackaging of particles in the mesopelagic zone of the subtropical and subarctic North Pacific Ocean. Deep. Res. Part II Top. Stud. Oceanogr. **55**: 1636–1647. doi:10.1016/j.dsr2.2008.04.019

Woodward, G., B. Ebenman, M. Emmerson, J. M. Montoya, J. M. Olesen, A. Valido, and P. H. Warren. 2005. Body size in ecological networks. Trends Ecol. Evol. **20**: 402–9. doi:10.1016/j.tree.2005.04.005

Zuur, A. F., E. N. Ieno, N. J. Walker, A. A. Saveliev, and G. M. Smith. 2009. Mixed Effects Models and Extensions in Ecology with R, M. Gail, K. Krickeberg, J.M. Samet, A. Tsiatis, and W. Wong [eds.]. Springer.

565 **Tables**

566 Table 1. Hydrographic conditions, pathways of organic matter OM and particle flux in each
567 BIOCANT cruise.

Oceanographic period	Cruise	Hydrographic conditions	Pathways of OM and particle flux
Onset spring bloom	March 2012, BIOCANT 1	High surface Chl *a* concentration. Vertical mixing.	Predominance of OM produced by phytoplankton in Surface Water (SW). Refractory suspended OM below SW from the previous production cycle and of terrigenous origin.
Late stratification	October 2012, BIOCANT 2	Low Chl *a* concentration. Thermocline of 6ºC gradient.	Suspended OM in the water column similar to the early stratification period (see below). Low mass flux.
Early stratification	May 2013, BIOCANT 3	Subsurface Chl *a* maximum. Thermocline of 2ºC gradient.	Suspended OM is homogeneous along the water column after the produced OM in the spring phytoplankton bloom has sank.

568

569

570 **Figures**

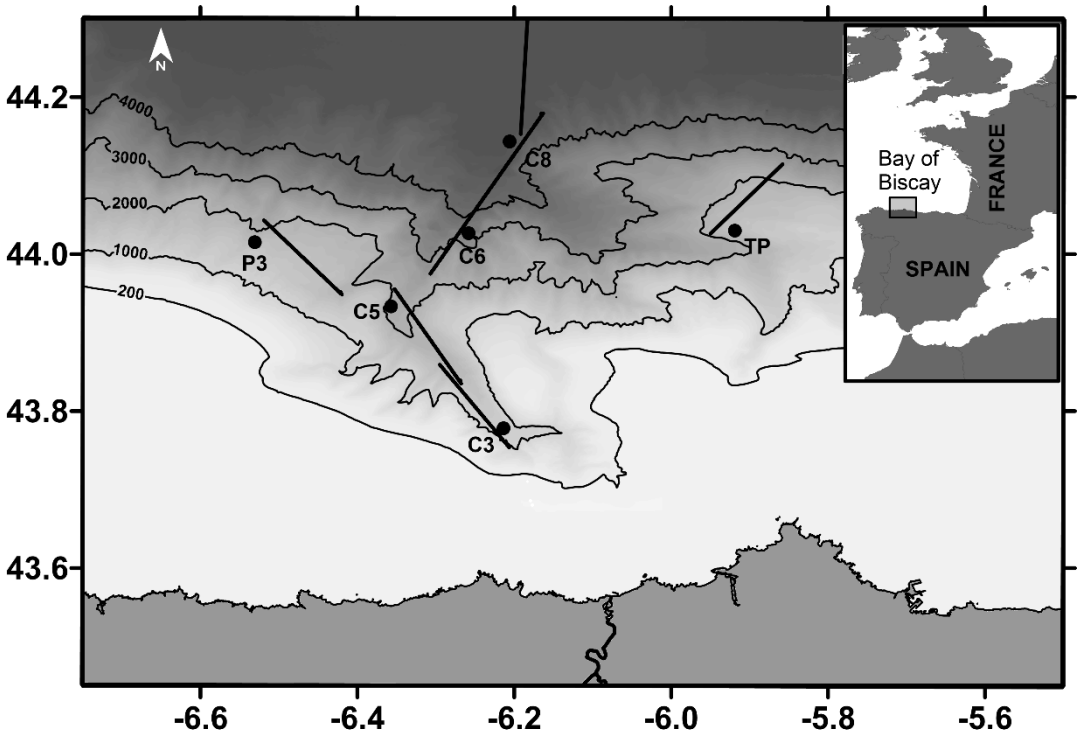

571

572 Figure 1. Map of the study area. Dots indicate locations of stations and lines refer to the

573 trawling of the MOCNESS net.

574

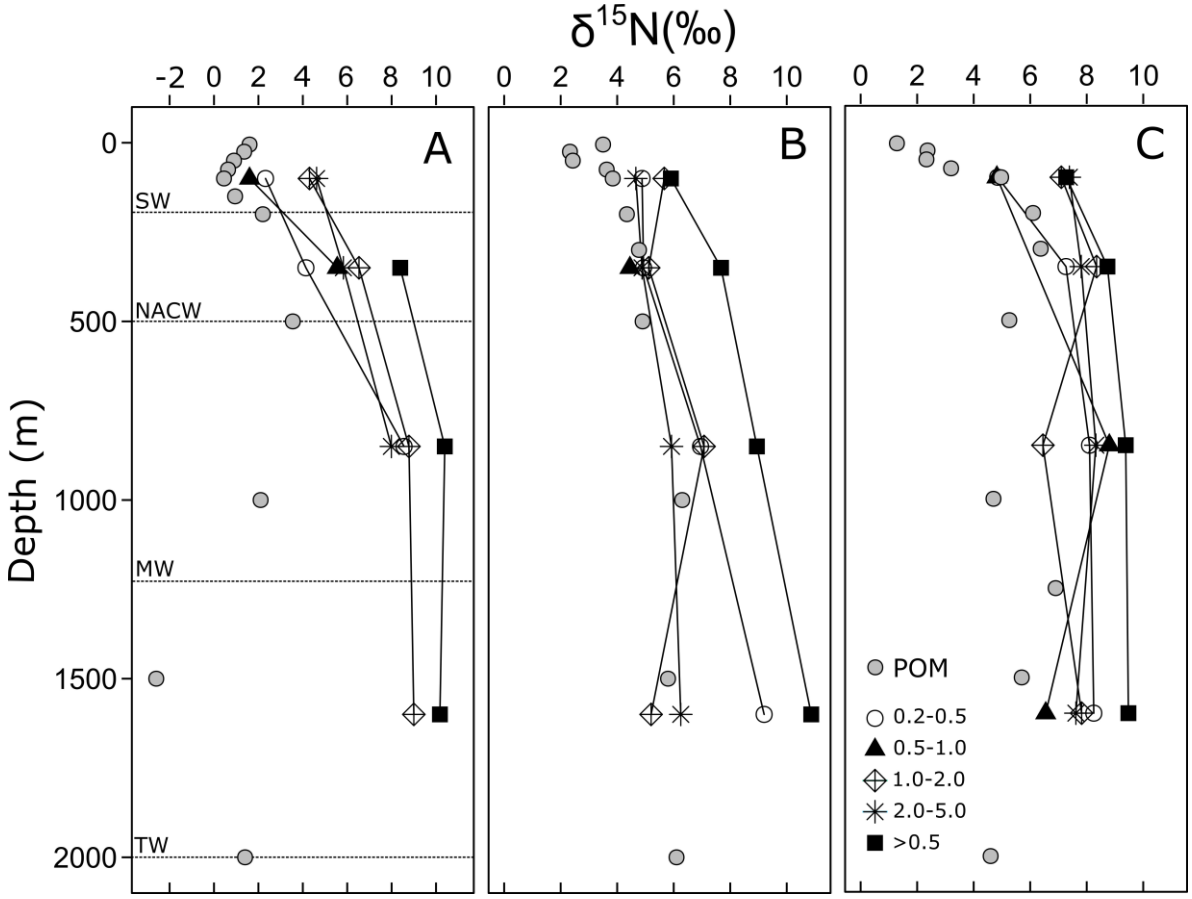

Figure 2. δ^{15}N values of size-fractionated zooplankton and suspended POM collected in each BIOCANT cruise: A) Onset of spring bloom, March 2012, BIOCANT 1; B) Early stratification, May 2013, BIOCANT 3; C) Late stratification, October 2012, BIOCANT 2. Each dot corresponds to the average between all stations at the mean depth of each water mass (SW: Surface Water; NACW: North Atlantic Central Water; MW: Mediterranean Water; TW: Transition Water). Horizontal dotted lines demarcate each water mass. Zooplankton size fractions are given in mm. Note different scale on x-axis.

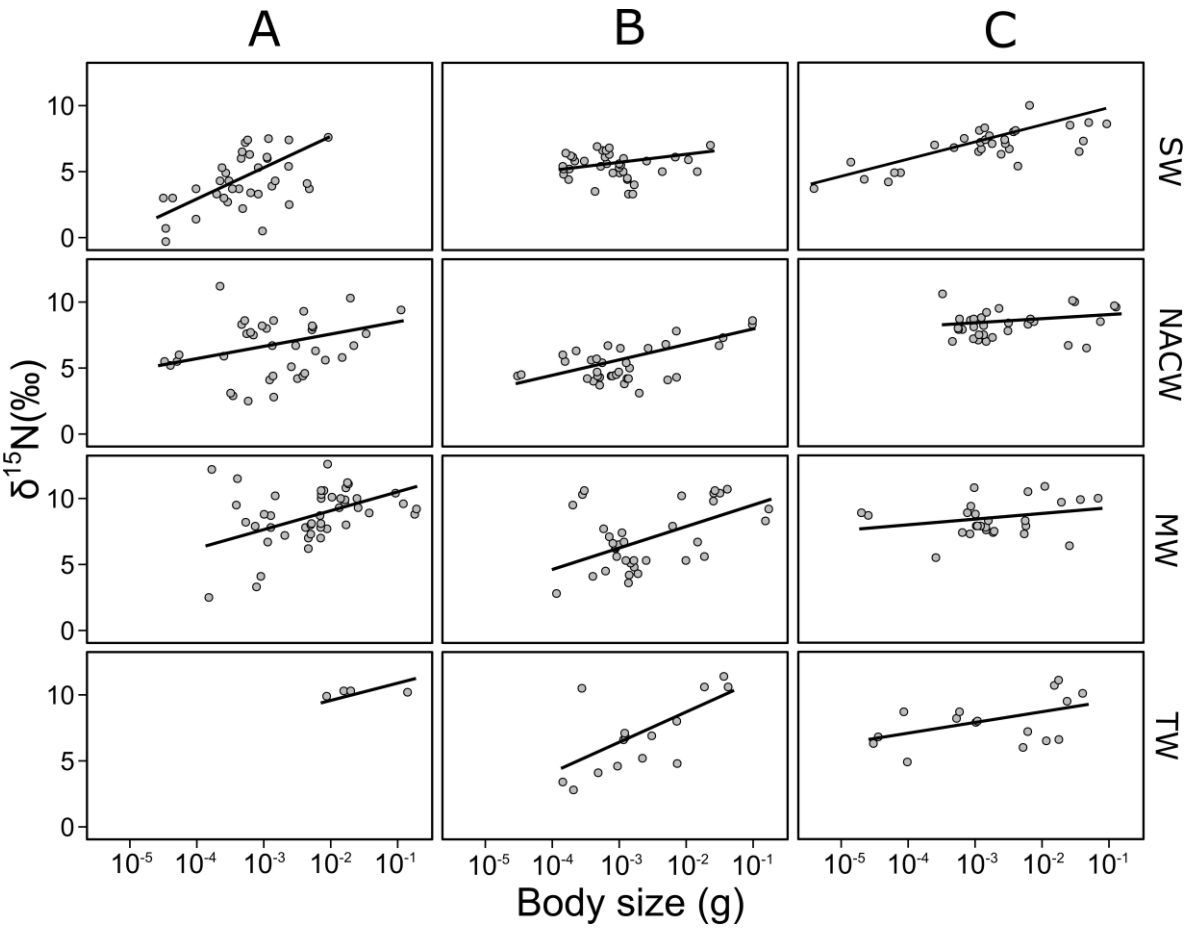

584

585 Figure 3. Relationship between $\delta^{15}N$ and $\log_{10}$ W for each cruise (A: Onset of spring
586 bloom, March 2012, BIOCANT 1; B: Early stratification, May 2013, BIOCANT 3; C: Late
587 stratification, October 2012, BIOCANT 2) and depth strata (SW: Surface Water; NACW:
588 North Atlantic Central Water; MW: Mediterranean Water; TW: Transition Water) fitted
589 from the selected linear mixed model (see material and methods section and Supporting
590 Information).

591

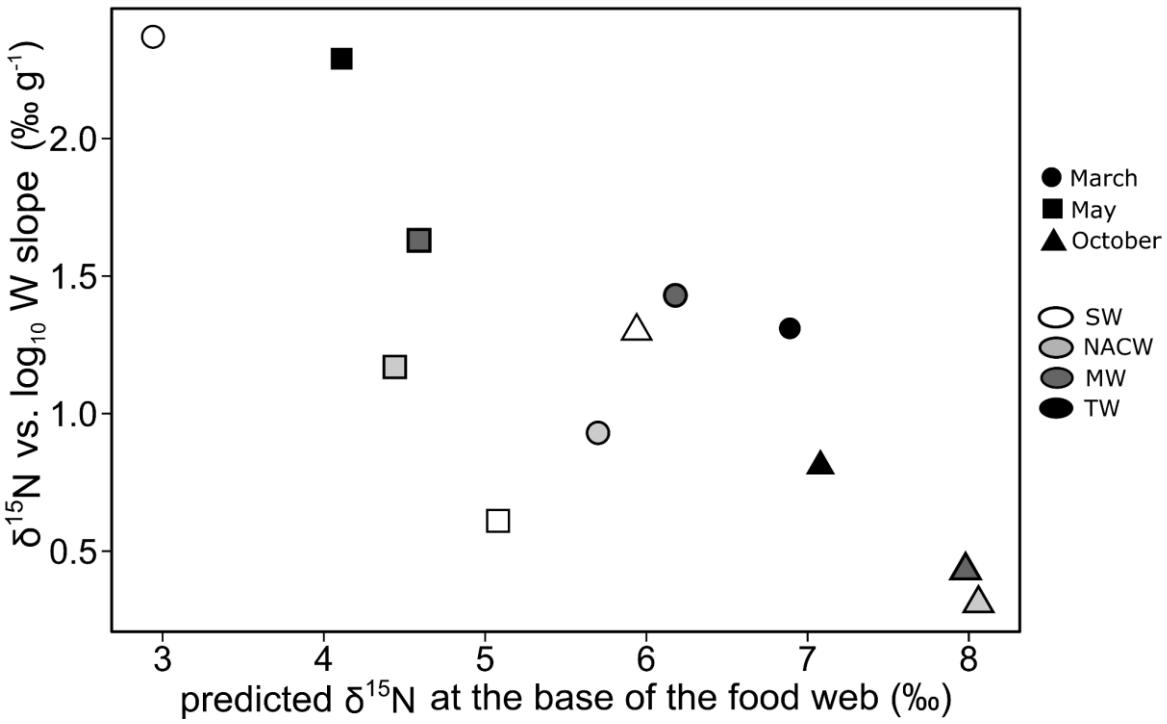

592

593 Figure 4. Slope and predicted δ^{15}N values for zooplankton at the base of the studied food
594 web (i.e. organisms weighing 10^{-4} g) estimated from the best model for the δ^{15}N vs. $\log_{10}$ W
595 relationship (Fig. 3) for each cruise (onset of spring bloom, March 2012, BIOCANT 1;
596 early stratification, May 2013, BIOCANT 3; late stratification, October 2012, BIOCANT
597 2) and depth strata (SW: Surface Water; NACW: North Atlantic Central Water; MW:
598 Mediterranean Water; TW: Transition Water).